VIP Zeolites Very Important Paper

International Edition: DOI: 10.1002/anie.201506822
German Edition: DOI: 10.1002/ange.201506822

# Direct Dual-Template Synthesis of MWW Zeolite Monolayers

*Vicente J. Margarit, Marta E. Martínez-Armero, M. Teresa Navarro, Cristina Martínez, and Avelino Corma**

***Abstract:*** *A two-dimensional zeolite with the topology of MWW sheets has been obtained by direct synthesis with a combination of two organic structure-directing agents. The resultant material consists of approximately 70% single and double layers and displays a well-structured external surface area of about 300 $m^2 g^{-1}$. The delaminated zeolite prepared by means of this single-step synthetic route has a high delamination degree, and the structural integrity of the MWW layers is well preserved. The new zeolite material displayed excellent activity, selectivity, and stability when used as a catalyst for the alkylation of benzene with propylene and found to be superior to the catalysts that are currently used for producing cumene.*

The importance of zeolites as adsorbents and heterogeneous catalysts is well recognized.[1] When used as catalysts, the microporous structure of these crystalline solids provides the reactants with a confined environment that, aside from preactivating the molecules, may direct the reaction towards the formation of the desired products by stabilizing the reaction transition states. However, the narrow pore dimensions of most zeolites, in the range of 4 to 7 Å, limit their use to processes involving relatively small molecules. Many efforts have been directed towards increasing the accessibility to the active sites and reducing the diffusional problems of bulkier reactants while preserving a certain degree of confinement. Traditionally, the accessibility to the active sites has been increased by means of post-synthetic methods that combine acid and hydrothermal treatments, such as in ultra-stabilized Y-based catalysts for fluid catalytic cracking (FCC)[2] or mordenite-based catalysts for hydroisomerization,[1,3] or by combining acid and base treatments.[4] These top-down procedures are effective but enclose several steps and, depending on the conditions employed, may result in the loss of crystallinity and micropore volume. The addition of soft or hard templates to the synthesis gel has also been described as a possible route to obtain hierarchical zeolites with micro- and mesoporosity.[4b,5] The direct synthesis of single layers of ZSM-5 was achieved by using diquaternary ammonium surfactants and tetraalkylphosphonium compounds as organic structure-directing agents (OSDAs).[6] The use of these types of OSDAs has also allowed the synthesis of other micro/mesoporous zeolites with structural mesoporosity[7] or intercrystalline mesoporosity that is due to small crystallite sizes.[8]

A different approach for increasing the accessibility of zeolites was described in the mid-1990s and involved the delamination of layered zeolite precursors. The concept was shown to be applicable to different structures, and the new delaminated zeolites ITQ-2,[9] ITQ-6,[10] ITQ-18,[11] and ITQ-20[12] were prepared starting from MCM-22(P), PRE-FER, NU-6(1), and ITQ-19, respectively.[13] The resultant zeolitic materials had very large accessible surface areas and displayed interesting catalytic properties in a large number of reactions.[14] The first of those delaminated zeolites, ITQ-2, is formed by disordered MWW layers in a "house of cards" disposition. The layers, with a thickness of 2.5 nm, present a hexagonal array of "cups" penetrating into the sheets from both sides, which consist of twelve-membered rings and are connected by a ten-ring channel running through the center of the layer.[9a] The preservation of the structure of the layers was improved by delaminating under milder conditions.[15] A certain degree of delamination in zeolite precursor MCM-22(P) has recently been achieved by treating the layered precursor with cetyltrimethylammonium bromide, tetrabutylammonium fluoride, and tetrabutylammonium chloride at a mild pH of 9.[16] The material obtained, UCB-1, presented high structural integrity, and the formation of amorphous silica phases was not been detected.

Herein, we present the single-step direct synthesis of a material containing a large proportion of MWW monolayers. The layered zeolite, hereafter referred to DS-ITQ-2, was obtained by using a combination of hexamethyleneimine (HMI), the traditional organic compound used for the synthesis of MWW materials, and a bifunctional OSDA, namely *N*-hexadecyl-*N'*-methyl-DABCO, ($C_{16}DC_1$; see Figure 1). We were expecting HMI to direct the crystallization of the MWW layers, whereas the cationic head of the $C_{16}DC_1$ molecule, which, according to $^{13}C$ MAS NMR spectroscopy, remains stable under the reaction conditions employed (see the Supporting Information, Figure S1), was expected to be located in the hemi-cavities of the layers while

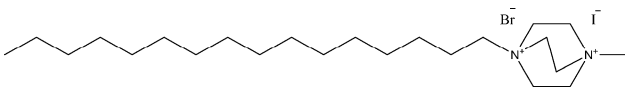


***Figure 1.*** The organic structure-directing agent $C_{16}DC_1$ used for the direct synthesis of delaminated MWW DS-ITQ-2.

[*] V. J. Margarit, M. E. Martínez-Armero, Dr. M. T. Navarro, Dr. C. Martínez, Prof. A. Corma
Instituto de Tecnología Química
Universidad Politécnica de Valencia
Consejo Superior de Investigaciones Científicas (UPV-CSIC)
Valencia, 46022 (Spain)
E-mail: acorma@itq.upv.es
Prof. A. Corma
King Fahd University of Petroleum and Minerals
P.O. Box 989, Dhahran 31261 (Saudi Arabia)

Supporting information for this article is available on the WWW under http://dx.doi.org/10.1002/anie.201506822.

  

the alkyl chain would avoid the layers to grow and order along the *c* axis. We will show that this synthesis route allows the one-step preparation of a delaminated zeolite with a high delamination degree and high structural preservation of the microporous layers.

The layer arrangement in MWW materials and their interlayer interactions can be deduced from the 6–10° 2$\theta$ range (Cu K$\alpha$ radiation) of their powder X-ray diffraction (XRD) patterns,[17] which are shown in Figure 2 for the as-

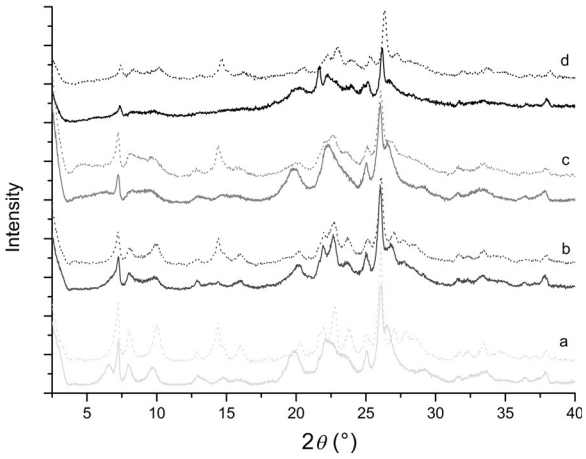


***Figure 2.*** XRD patterns for MCM-22 (a), MCM-56 (b), DS-ITQ-2 (c), and ITQ-2 (d), as-prepared (——) and calcined (-----).

prepared (——) and calcined (-----) samples. MCM-22(P) presents a doublet in the lower 6.5–7° 2$\theta$ region ((002) is the interlayer reflection and (100) the intralayer one). Upon calcination, the (002) peak is shifted to higher 2$\theta$ angles and overlaps with the (100) peak. Both MCM-22(P) and MCM-22 present two discrete peaks at 2$\theta$ values of 8.1 and 10°, which are due to the interlayer reflections (101) and (102), indicating stacking with 3D order. The XRD pattern obtained for MCM-56,[18] one of the disordered materials of the MWW family obtained by direct synthesis, corresponds to that of a zeolite with partial condensation of the MWW sheets and a large proportion of layers randomly translated in the *ab* plane and submerged within each other.[17b] In the case of ITQ-2, the XRD patterns present a unique, broad band in the 7.5–10° 2$\theta$ range, confirming the disordered arrangement of its layers and a high delamination degree. However, with the direct synthesis presented here, the structural integrity of the MWW layers of the highly delaminated zeolite, associated with the intensity of the 2$\theta$ peak at 7.1° (100), is clearly higher than for the delaminated ITQ-2 material prepared by post-synthetic methods. The thermal stability of the new material is high, as can be deduced from the preservation of the XRD patterns corresponding to the as-prepared and the calcined samples.

The higher degree of crystallinity of the material prepared here as compared to conventional ITQ-2 was also confirmed by the shape of the Ar and $N_2$ adsorption isotherms of the corresponding calcined samples (see Figures 3 and S2, respectively). These are closer to a type I, representative of

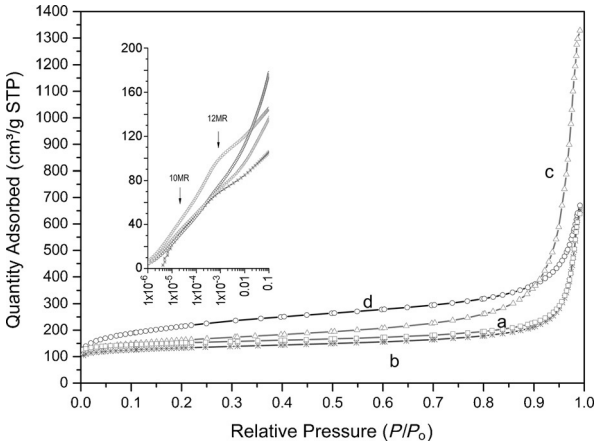


***Figure 3.*** Argon adsorption isotherms of the calcined MWW materials: a) MCM-22, b) MCM-56, c) DS-ITQ-2, and d) ITQ-2. Inset: enlargement of the low relative pressure region.

microporous materials (MCM-22), than to a type IV isotherm, which is typical of disordered mesoporous materials (ITQ-2), at relative pressures of up to 0.5. However, at $P/P_0 >$ 0.8, the sharp increase in adsorption indicates an extremely high total pore volume of the material prepared in one step (2.06 $cm^3 g^{-1}$) that is twice the values determined for MCM-56 or conventional ITQ-2 (see Table S1). Moreover, at low relative pressures, the Ar adsorption isotherms show the inflection points corresponding to the ten-ring channels and twelve-ring supercages for MCM-22, and the absence of the latter for conventional ITQ-2, as described previously[9c] (see Figure 3, inset). Regarding the newly prepared material, the inflection at the lowest $P/P_0$ value is more intense than that of ITQ-2, indicating a better preservation of the layered structure when the delaminated MWW is obtained by this new one-step procedure. The high delamination degree was confirmed by the significant reduction in the inflection of the 12-MR cavities.

The DS-ITQ-2 material has a larger external surface area than MCM-22 and MCM-56, although it is smaller than for ITQ-2. However, its higher micropore volume is an additional indication of the larger structural integrity of the MWW layers as compared to the delaminated zeolites obtained by post-synthetic treatments.

The morphology of the zeolite material prepared here is different from that of MCM-22 or the post-synthesis-delaminated ITQ-2 according to the SEM images shown in Figure 4. Although the crystals have a platelet shape in all cases, DS-ITQ-2 presents an open and vertical disposition of well-defined small crystallites, whereas they are more agglomerated for conventional ITQ-2.

Definite evidence for the presence of individual layers is given by the HRTEM images shown in Figure 5, where the high delamination degree is clearly visible. To evaluate the degree of delamination in this new material, we analyzed 30 different HRTEM images and 275 different crystals. This detailed investigation gave the distribution presented in Figure S3, which has been obtained considering a layer thickness of 2.5 nm. Most of the crystals are mono- (34%)

  

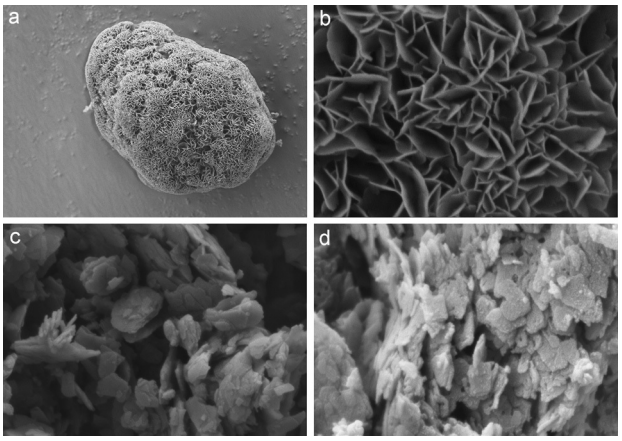


***Figure 4.*** SEM images of calcined MWW materials: a, b) DS-ITQ-2, c) MCM-22, and d) ITQ-2.

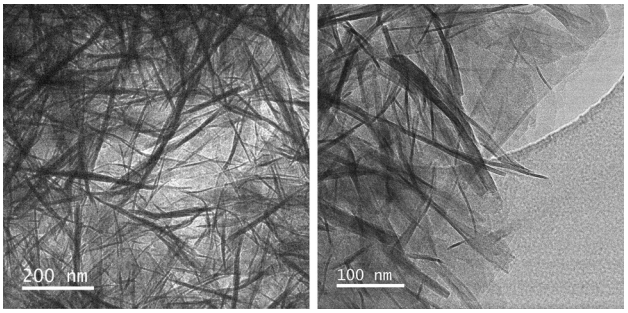


***Figure 5.*** HRTEM images of calcined DS-ITQ-2.

or bilayered (36%), whereas only 9% of the crystals measured consist of more than three sheets.

The thermal stability of the DS-ITQ-2 zeolite can be deduced from the preservation of the structure according to the XRD pattern of the calcined sample (Figure 2) and its micropore volume (see Table S1). As determined by $^{27}$Al MAS NMR spectroscopy (Figure 6), the proportion of Al remaining in framework positions in the calcined sample is close to 80% and thus in the same range as that observed for MCM-22 or conventional ITQ-2 (Figure S4a). This percentage is significantly higher than that of disordered zeolite MCM-56, where 30% of the Al atoms are found in

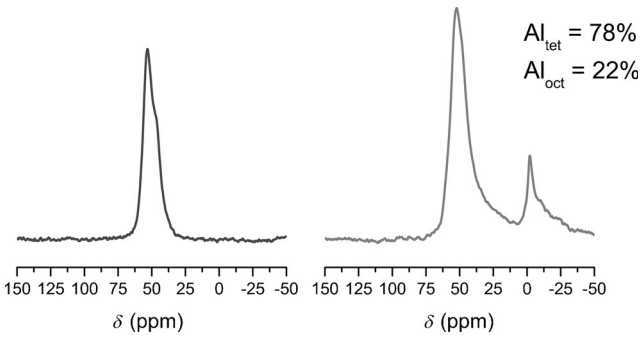


***Figure 6.*** $^{27}$Al MAS NMR spectra of as-prepared (left) and calcined (right) DS-ITQ-2.

octahedrally coordinated extra-framework positions after thermal treatment.

The Brønsted acidity related to the presence of framework Al atoms was studied by FT-IR spectroscopy in combination with the adsorption of two probe molecules of different size. The smaller pyridine is able to enter the micropores of all samples; it can interact with all Brønsted acidic sites in the zeolites, and will give information on the total Brønsted acid site density (see Figure S5a). The bulkier di-*tert*-butyl-pyridine (DTBP) will be able to interact only with the external sites, located at the external cups, but not with the acid sites within the circular ten-ring channels with the acid sites located within the large twelve-ring cavities connected by the ten-ring channels (see Figure S5b).

The FT-IR spectra of the four MWW samples after pretreatment at 400 °C under vacuum (——) and after adsorption of the basic probe (– – –) are shown in Figure 7. Results

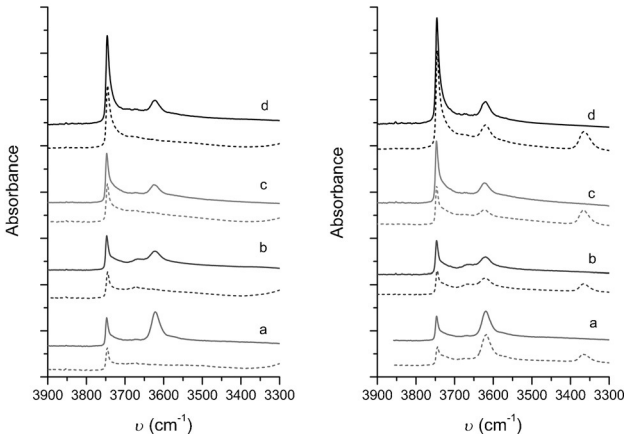


***Figure 7.*** FT-IR spectra of the calcined MWW materials pretreated at 400 °C under vacuum (——) and after adsorption of the probe molecules (– – –) pyridine (left) or DTBP (right). a) MCM-22, b) MCM-56, c) DS-ITQ-2, d) ITQ-2.

obtained for the adsorption of pyridine and DTBP are shown on the left and right, respectively. Two main bands at 3750 and at 3620 cm$^{-1}$ were observed for the four zeolites before adsorption of the probes, which were assigned to external silanol and acidic hydroxy groups, respectively.

The new DS-ITQ-2 sample has a similar Brønsted acid site density to conventional ITQ-2 (see Figure 7 and Table S2), but less external silanol groups. This finding confirms that the layer structure is preserved to a larger extent in the former zeolite, which displays a smaller amount of defects, but also a lower external surface area; these results are in agreement with the textural properties given in Table S1.

The interaction of pyridine with the Brønsted acid sites was in all cases confirmed by the disappearance of the 3620 cm$^{-1}$ band, which had been assigned to acidic hydroxy groups. However, the improved accessibility of ITQ-2 and the new delaminated material was confirmed by the interaction of a larger amount of Brønsted acid sites with the bulkier DTBP as compared to MCM-22 or MCM-56, where the decrease in

  

the intensity of the 3620 $cm^{-1}$ band after adsorption of the bulkier basic molecule is considerably smaller (see Figure 7 and Table S2).

The alkylation of benzene with propene is an industrial process for obtaining cumene, an intermediate in the production of phenol and acetone.[1,19] The current trend is to operate in the liquid phase and in the presence of zeolite-based catalysts. The zeolites employed are generally large-pore materials, such as Beta zeolite, with no restrictions for cumene diffusion through the 12 MR pores. MCM-22, which presents an unexpected good catalytic behavior that is comparable to, if not better than, that of the large-pore zeolites, is also employed. Different studies confirmed that only the external surface of MCM-22 was participating in the reaction,[20] and delaminated ITQ-2 was in fact shown to have a higher activity and a substantially improved catalyst lifetime compared to MCM-22.[21]

The catalytic behavior of the new MWW material in the liquid-phase alkylation of benzene with propene to cumene is the final confirmation of the exceptional properties of this delaminated zeolite obtained by a single-step procedure. Despite its lower external surface area, its initial activity is comparable to that of conventional ITQ-2 for a wide range of space velocities and significantly higher than that of MCM-22 or MCM-56, especially at the highest space velocities considered (Figure 8a). The main difference when compared with MCM-22 and MCM-56 is the deactivation rate (see Figure 8b and Figure S6).

The variation of the conversion with time on stream (see Figure S6 for two different space velocities, 50 and 100 $h^{-1}$) can be described by the first-order deactivation relation given in Eq. (1),[22] where $X$ and $X_0$ are the initial and subsequent propene conversion values, $t$ is the time on stream, and $k_D$ is the deactivation constant.

$$X = X_0\, e^{(-k_D t)} \quad (1)$$

The deactivation constants thus obtained (plotted in Figure 8b) are significantly lower for the delaminated DS-ITQ-2 and ITQ-2 materials than for MCM-22 or MCM-56. Regarding the product selectivity, the results for the four samples are in the same range when plotted versus conversion (see Figure S7). This finding is in line with the fact that only the external sites are involved in the acid-catalyzed alkylation reaction.

In summary, we have presented a new single-step route for the direct synthesis of a delaminated MWW material with a high delamination degree and high structural preservation of the microporous layers. For the first time, a MWW material, which consisted of more than 70% mono- and bilayered crystals, was obtained by direct synthesis in high yield (78%). The synthesis was enabled by the combination of two different organic structure-directing agents, namely HMI for the crystallization of the microporous layers and a bifunctional biquaternary ammonium surfactant for avoiding the growth and stacking of the layers along the $c$ axis. DS-ITQ-2 showed the same catalytic activity, selectivity, and stability towards deactivation on stream as the reference catalyst ITQ-2, which was obtained following the traditional post-synthesis delamination procedure, but benefits from the advantages of a single-step synthesis procedure and a larger zeolite yield.

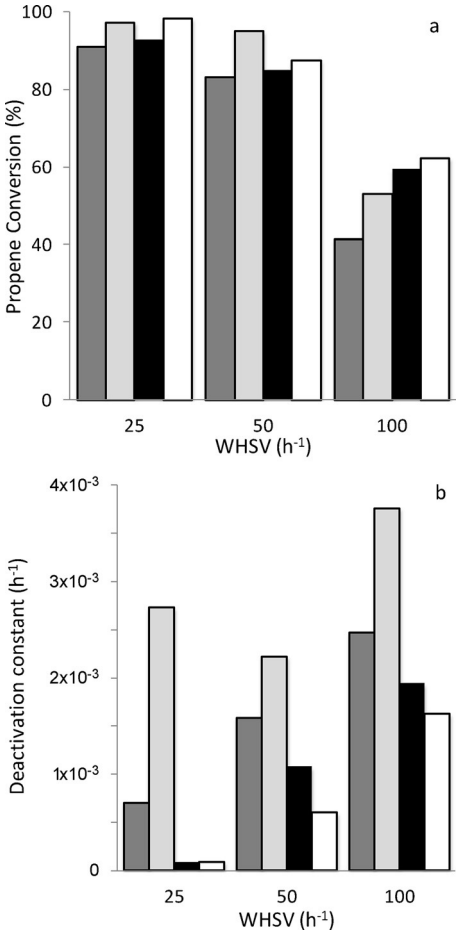


***Figure 8.*** Initial activity (top) and deactivation constant (bottom) for MCM-22 (■), MCM-56 (■), DS-ITQ-2 (■), and ITQ-2 (□) for the liquid-phase alkylation of benzene with propene at different space velocities. Weight hourly space velocity (WHSV) = 25, 50, or 100 $h^{-1}$, $T$ = 398 K, $P$ = 3.5 MPa.

## *Experimental Section*

DS-ITQ-2 was prepared by dissolving $NaAlO_2$ (0.846 g; 47% $Al_2O_3$, 34.4% $Na_2O$, 18.6% $H_2O$, Carlo Erba) and NaOH (10.460 g, 10% in water) in doubly distilled water (46.428 g). Then, $C_{16}DC_1$ (6.713 g) was added to the solution while stirring. When the surfactant had been completely dissolved, hexamethyleneimine (3.713 g; Sigma–Aldrich) and fumed silica (7.210 g; Sigma–Aldrich, particle size = 0.007 μm) were added to the mixture, which was stirred vigorously for 1 h to obtain a gel with a molar $Na_2O/SiO_2/Al_2O_3/HMI/C_{16}DC_1/H_2O$ composition of 0.15:1:0.033:0.3:0.1:40. Finally, the gel was transferred to a 35 mL PTFE-lined stainless-steel autoclave, which was rotated at 60 rpm and heated to 423 K for 7 days. After quenching the reaction mixture with cold water, the product was filtered, washed with distilled water until pH < 9, and dried at 373 K overnight. The organic material was removed by calcination in air at 813 K for 12 h.

MCM-22, MCM-56, and ITQ-2 were synthesized following the procedures described in the literature.[9a,18,23]

The acidic zeolites were used to catalyze the liquid-phase alkylation of benzene with propene at 398 K, 3.5 MPa, and a space velocity of 25–100 $h^{-1}$. The reaction was performed in a stainless-steel

  

fixed-bed reactor, and the composition of the outlet stream was analyzed on-line on a Varian-450 gas chromatograph equipped with a 30 m 5% phenyl/95% dimethylpolysiloxane capillary column connected to a flame ionization detector.

## Acknowledgements

Financial support by the Spanish Government-MINECO through "Severo Ochoa" (SEV 2012–0267), Consolider Ingenio 2010-Multicat, and MAT2012-31657 is acknowledged. M.E.M.-A. thanks MINECO for financial support through a pre-doctoral fellowship (BES-2013–066800).

**Keywords:** alkylation · cumene · heterogeneous catalysis · organic structure-directing agents · zeolites

**How to cite:** *Angew. Chem. Int. Ed.* **2015**, *54*, 13724–13728
*Angew. Chem.* **2015**, *127*, 13928–13932

[1] C. Martínez, A. Corma, *Coord. Chem. Rev.* **2011**, *255*, 1558.
[2] A. Corma, *Chem. Rev.* **1995**, *95*, 559.
[3] J. Lazaro, A. Corma, J. Frontela, U.S. Patent 5057471, **1991**.
[4] a) S. van Donk, A. H. Janssen, J. H. Bitter, K. P. de Jong, *Catal. Rev. Sci. Eng.* **2003**, *45*, 297; b) J. Pérez-Ramírez, C. H. Christensen, K. Egeblad, C. H. Christensen, J. C. Groen, *Chem. Soc. Rev.* **2008**, *37*, 2530.
[5] a) I. I. Ivanova, A. S. Kuznetsov, V. V. Yuschenko, E. E. Knyazeva, *Pure Appl. Chem.* **2004**, *76*, 1647; b) I. I. Ivanova, A. S. Kuznetsov, O. A. Ponomareva, V. V. Yuschenko, E. E. Knyazeva, *Stud. Surf. Sci. Catal.* **2005**, 158A, 121; c) V. V. Ordomsky, V. Y. Murzin, Y. V. Monakhova, Y. V. Zubavichus, E. E. Knyazeva, N. S. Nesterenko, I. I. Ivanova, *Microporous Mesoporous Mater.* **2007**, *105*, 101; d) J. Garcia-Martinez, C. Xiao, K. A. Cychosz, K. Li, W. Wan, X. Zou, M. Thommes, *ChemCatChem* **2014**, *6*, 3110; e) T. Prasomsri, W. Jiao, S. Z. Weng, J. Garcia Martinez, *Chem. Commun.* **2015**, *51*, 8900.
[6] a) M. Choi, K. Na, J. Kim, Y. Sakamoto, O. Terasaki, R. Ryoo, *Nature* **2009**, *461*, 246; b) X. Zhang, D. Liu, D. Xu, S. Asahina, K. A. Cychosz, K. V. Agrawal, Y. A. Wahedi, A. Bhan, S. A. Hashimi, O. Terasaki, M. Thommes, M. Tsapatsis, *Science* **2012**, *336*, 1684.
[7] W. Kim, J.-C. Kim, J. Kim, Y. Seo, R. Ryoo, *ACS Catal.* **2013**, *3*, 192.
[8] a) L. Wu, V. Degirmenci, P. C. M. M. Magusin, N. J. H. G. M. Lousberg, E. J. M. Hensen, *J. Catal.* **2013**, *298*, 27; b) J. Kim, C. Jo, S. Lee, R. Ryoo, *J. Mater. Chem. A* **2014**, *2*, 11905.
[9] a) A. Corma, V. Fornes, S. B. Pergher, T. Maesen, J. G. Buglass, *Nature* **1998**, *396*, 353; b) A. Corma, V. Fornes, J. Martinez-Triguero, S. B. Pergher, *J. Catal.* **1999**, *186*, 57; c) A. Corma, V. Fornes, J. M. Guil, S. Pergher, T. L. M. Maesen, J. G. Buglass, *Microporous Mesoporous Mater.* **2000**, *38*, 301.
[10] a) A. Corma, U. Diaz, M. E. Domine, V. Fornes, *Chem. Commun.* **2000**, 137; b) A. Corma, U. Diaz, M. E. Domine, V. Fornes, *Angew. Chem. Int. Ed.* **2000**, *39*, 1499; *Angew. Chem.* **2000**, *112*, 1559; c) A. Corma, U. Diaz, M. E. Domine, V. Fornes, *J. Am. Chem. Soc.* **2000**, *122*, 2804.
[11] A. Corma, V. Fornes, U. Diaz, *Chem. Commun.* **2001**, 2642.
[12] A. Corma Canós, U. Díaz Morales, V. Fornes Segui, Consejo Superior de Investigaciones Cientificas (Madrid, Spain), Universidad Politecnica de Valencia (Valencia, Spain) **2006**.
[13] U. Díaz, A. Corma, *Dalton Trans.* **2014**, *43*, 10292.
[14] a) A. Corma, V. Gonzalez-Alfaro, A. V. Orchilles, *Appl. Catal. A* **1999**, *187*, 245; b) A. Corma, H. Garcia, J. Miralles, *Microporous Mesoporous Mater.* **2001**, *43*, 161; c) C. González-Arellano, A. Corma, M. Iglesias, F. Sanchez, *Adv. Synth. Catal.* **2004**, *346*, 1758; d) M. J. Climent, A. Corma, A. Velty, *Appl. Catal. A* **2004**, *263*, 155.
[15] a) S. Maheshwari, E. Jordan, S. Kumar, F. S. Bates, R. L. Penn, D. F. Shantz, M. Tsapatsis, *J. Am. Chem. Soc.* **2008**, *130*, 1507; b) S. Maheshwari, C. Martinez, M. T. Portilla, F. J. Llopis, A. Corma, M. Tsapatsis, *J. Catal.* **2010**, *272*, 298.
[16] I. Ogino, M. M. Nigra, S. J. Hwang, J. M. Ha, T. Rea, S. I. Zones, A. Katz, *J. Am. Chem. Soc.* **2011**, *133*, 3288.
[17] a) W. J. Roth, D. L. Dorset, *Microporous Mesoporous Mater.* **2011**, *142*, 32; b) M. Polozij, H. V. Thang, M. Rubes, P. Eliasova, J. Cejka, P. Nachtigall, *Dalton Trans.* **2014**, *43*, 10443.
[18] A. S. Fung, S. L. Lawton, J. Roth, U.S. Patent 5362697, **1994**.
[19] a) W. Vermeiren, J.-P. Gilson, *Top. Catal.* **2009**, *52*, 1131; b) P. Beltrame, G. Zuretti, *Green Chem.* **2004**, *6*, 7.
[20] a) G. Sastre, C. R. A. Catlow, A. Corma, *J. Phys. Chem. B* **1999**, *103*, 5187; b) C. Perego, R. Millini, W. O. Parker, Jr., G. Bellussi, U. Romano, *Stud. Surf. Sci. Catal.* **2004**, *154C*, 2239.
[21] P. J. Van den Brink, A. Corma Canos, E. J. Creyghton, V. Fornes Segui, V. Martinez Soria, WO 2001/021562, **2001**.
[22] A. Voorhies, *Ind. Eng. Chem. Res.* **1945**, *37*, 318.
[23] M. K. Rubin, P. Chu, U.S. Patent 4954325, **1990**.

Received: July 23, 2015
Published online: September 17, 2015

  